

Article

Study on the Mechanism and Prevention of Frequent Mine Seismic Events in Goaf Mining under a Multi-Layer Thick Hard Roof: A Case Study

Bo Wang^{1,2,3,4} , Guorui Feng^{1,3,*}, Zhongxiang Gao², Junpeng Ma², Sitao Zhu⁴ , Jinwen Bai^{1,3}, Zhu Li^{1,3} and Wenda Wu^{1,3}

¹ College of Mining Technology, Taiyuan University of Technology, Taiyuan 030024, China

² Yankuang Energy Group Co., Ltd., Jining 273500, China

³ Key Laboratory of Shanxi Province for Mine Rock Strata Control and Disaster Prevention, Taiyuan 030024, China

⁴ School of Civil and Resource Engineering, University of Science and Technology Beijing, Beijing 100083, China

* Correspondence: fguorui@163.com

Abstract: Mine seismic events are an inevitable dynamic phenomenon occurring in deep mines. A scientific and rational method is needed to evaluate and understand mine seismicity and its induced disasters. In the Ordos mining area of North China, multiple groups of thick hard-bedded sandstone formations commonly exist in the overlying strata of Jurassic coal seams. In recent years, frequent mine seismic events in many large mines of Ordos have resulted in suspended or limited production, which seriously threatens the safe and efficient operation of 10-million-ton modern mines in China. Therefore, taking the frequent occurrence of mine seismic events in the mining process of goaf working face with a multi-layer thick hard roof in Ordos mine as the research background, this study investigated the mechanism and prevention of mine seismic in goaf working face with the methods of case study, theoretical analysis and field monitoring. The following conclusions are made: when the goaf working face is mined, an “advanced and lateral” L-form roof forms under the coupled influence of the lateral suspension plate formed above the upper working face and the roof of the working face. Due to the common influence from “advanced and lateral” L-form roof activation, the gradually breaking multi-layer thick hard roof, thick hard roof group bending and prying effects, in addition to excessively fast or uneven mining speed, mine seismic events will occur frequently when the exceedance warning index (EWI) is breached. On this basis, coordinated blasting to break the roof along two roadways and within the working face is put forward as a measure with the purpose of preventing and controlling mine seismic events, and a robust effect on mine seismic reduction and disaster prevention is obtained in field application. The research results can serve as a reference for the development and application of mine seismic mechanism and blasting vibration reduction technology on the working face where there is a multi-layer thick hard roof, thereby supporting a strategy of promoting the resource development and energy security of deep mines.

Keywords: multi-layer thick hard roof; mine seismic; overlying strata movement; gradual fracture failure; roof blasting; energy and frequency



Citation: Wang, B.; Feng, G.; Gao, Z.; Ma, J.; Zhu, S.; Bai, J.; Li, Z.; Wu, W. Study on the Mechanism and Prevention of Frequent Mine Seismic Events in Goaf Mining under a Multi-Layer Thick Hard Roof: A Case Study. *Minerals* **2023**, *13*, 852. <https://doi.org/10.3390/min13070852>

Academic Editor: Abbas Taheri

Received: 9 May 2023

Revised: 9 June 2023

Accepted: 21 June 2023

Published: 23 June 2023



Copyright: © 2023 by the authors. Licensee MDPI, Basel, Switzerland. This article is an open access article distributed under the terms and conditions of the Creative Commons Attribution (CC BY) license (<https://creativecommons.org/licenses/by/4.0/>).

1. Introduction

Underground mineral resources are an important material basis for human economic and social development, and “seeking resources from underground” is an important way to maintain sustainable development [1–6]. For mines entering into the deep mining stage, the geological conditions and stope structure become more complex, dynamic disasters significantly increase in terms of frequency and degree of damage and more mines will be threatened by dynamic disasters such as mine seismic events and rock burst [7–12]. Ordos Basin is an important coal production base in China, characterized by multiple

groups of thick hard-bedded sandstone formations in the overlying strata of its main coal seam [13]. With the continuous expansion of mining scope, large-energy mine seismic events frequently take place, especially on the goaf working face, and mine seismic events and rock burst have appeared in several mines [14], as shown in Figure 1. Figure 1b–d are examples of serious damage to mines, with the blocked safety exit of the return air roadway in Hulusu Mine [15], 16 bent single pillars of the goaf roadway in Menkeqing Mine and a subsiding roof in Nalinhe Mine [16]. These dynamic disasters have seriously restricted the safe and efficient production of the Ordos mining area. Therefore, an in-depth study on the occurrence mechanism of frequent mine seismic events under the condition of having a multi-layer thick hard roof is critical to ensure the sustained development of deep coal resources.

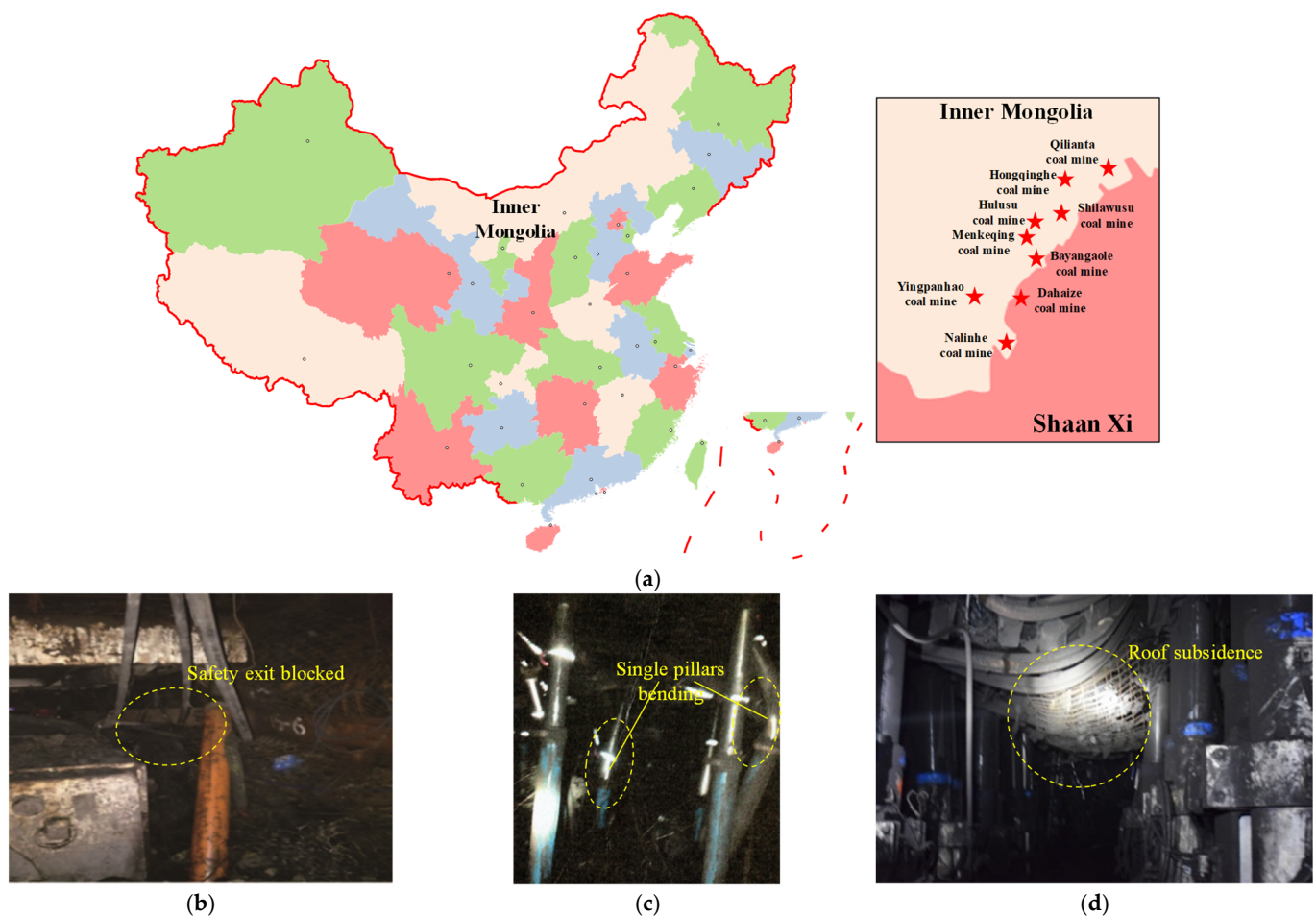


Figure 1. Overview of mine seismic events and dynamic disasters in Ordos mining area of China: (a) location of Ordos mining area [17]; (b) safety exit blocked in Hulusu Mine; (c) bending of single pillars in Menkeqing Mine; (d) roof subsidence in Nalinhe Mine.

Precise analysis of the mechanism of mine seismicity and its prevention and control are prerequisites for preventing dynamic disasters such as mine seismic events and rock burst. Scholars both in China and around the world have carried out extensive investigations on the mechanisms underlying mine seismic events. Dou et al. [18,19] comprehensively analyzed the characteristics of massive mine seismic information, such as mine seismic wave characteristics, wave velocity and underground ore pressure appearance, where mine seismic events were divided into three types (namely, mining fracture, ultra-thick overburden and high-energy mine seismicity) and conducted studies on the attenuation law of mine seismic in goaf. Cao et al. [14,20,21] explored the focal mechanism of large-energy mine seismic events induced by mining in a solid coal and a goaf section under a super-thick

overburden rock by quantitatively analyzing the evolution characteristics of roof rupture and how the orientation was affected by vibration wave radiation. Orlecka et al. [22] studied the influence of static load stress transfer caused by two strong mine seismic events occurring in the same mining area on subsequent mine seismic activities. Rudzinski et al. [23] determined the internal relationship between the foci location and mechanism of mine seismic events and the surface deformation above the collapsed tunnel. Wu et al. [24] investigated the mechanism of strong mine seismicity induced by the rupture of ultra-thick red strata, finding that both shear and tensile rupture of ultra-thick red strata could induce strong mine seismicity, but shear slip rupture was more likely to induce strong mine seismic manifestations of a mine tremor that can be felt on the Earth's surface. Mendecki et al. [25] explored the release law of microseismic energy in front of the working face before the occurrence of strong mine seismicity. He et al. [26] studied the mechanism of strong mine seismicity induced by the breaking of a thick hard roof at different positions and concluded that the roof breaking of goaf in the middle of the working face was prone to tensile rupture. Steck et al. [27] determined the mechanical conditions causing high-energy mine seismic events by analyzing the focal mechanism parameters. Xue et al. [28] analyzed the change characteristics of the energy ratio between S wave and P wave in the vibration signal of strong mine seismicity, finding that the coal rock mass experienced different damage modes during the preparation process of strong mine seismic. Xu et al. [29] concluded that the breaking motion of thick and hard rock strata was the main reason behind the induction of strong mine seismic events and discussed the stress and energy evolution characteristics during the breaking of thick and hard rock strata. Wu et al. [30] studied the spatio-temporal activity of microseismic large-energy events in the initial transition stage of coal pillar width conversion in the Hujilt mining area.

On the basis of mine seismic prevention and control, Zhu et al. [31] and Shang et al. [32,33] established the energy prediction model of rooftop mine seismic events based on the "movement state of key strata", with the calculation of rooftop mine energy, and proposed a method for preventing and controlling mine seismicity in the massive and thick hard rock by hydraulic fracturing in vertical wells. Cui et al. [34] studied the distribution characteristics of microseismic large-energy events on the mining face under solid coal and goaf and determined the relationship between microseismic large-energy events and the distribution law of mine pressure. Gao et al. [35] calculated the energy value during the first and periodic fracture of the source layer and the energy dissipation mechanism of the shock wave within this process and analyzed the near- and far-field effects of the shock source layer energy level on the impact of mining space mining earthquake under conditions of thick and hard overburden. In that paper, an idea was introduced for preventing mine seismicity via ground-underground stereo cooperation of high and low levels for rock fracturing and energy release. Lai et al. [36] clarified the energy migration path affected by mining depth according to the cluster analysis of microseismic events and formed a concept and strategy of dynamic disaster prevention for steep and thick coal seam. Yu and Gao et al. [37,38], aiming at the development of strategies to control the problems of strong strata pressure caused by mining of an ultra-thick coal seam with a hard roof, proposed the underground near-field precracking and hard rock weakening technology of surface far-field fracturing to control the development of strong strata pressure on the working face. Qin et al. [39] investigated the mechanism of mine seismicity in the roadway of solid coal in deep buried structural area and proposed a method to prevent mine seismicity by using advanced long distance drilling pressure relief. Wen et al. [40] studied the frequent occurrence of large-energy mine seismic events caused by the weakly consolidated thick roof breaking of wide coal pillars, determined the horizon of large-energy mine seismic occurrence and roof pressure relief by deep-hole blasting, and proposed a targeted pressure relief blasting scheme. Pan et al. [41] put forward a method of "artificial liberated layer" for the pressure relief and prevention of mine seismicity in the thick and hard roof area of the main disaster zone above the coal seam that was created by hydraulic fracturing.

It can be seen that the above scholars researched mechanisms for the occurrence and measures for the prevention of large-energy mine seismic events and achieved fruitful results. However, most studies examined single-influence conditions or a single large-energy mine seismic event, and investigations into the frequent occurrence of large-energy mine seismic events are lacking. Therefore, taking the frequent occurrence of mine seismic events in the mining process of goaf working face with a multi-layer thick hard roof in Ordos mine as the research background, this study investigates the distribution characteristics and key influencing factors of large-energy mine seismic events over several months with the methods of case study, theoretical analysis and field monitoring, further proposing the measure of coordinated blasting to break the roof along two roadways and within the working face. The aim is to provide a reference for the prevention and control of coal seam mining earthquake under similar roof conditions in the Ordos mining area, effectively preventing the occurrence of mine seismic events and other disasters and ensuring the sustainable development of deep coal resources.

2. Engineering Background

2.1. Field Conditions and Strata Structure of the 2215 Longwall Working Face

The 2215 longwall working face (LW2215) is the second mining face located in the south of mining area 22, where the north face is solid coal, and the south is near the goaf of the 2217 working face. The open-off cuts of the two working faces are flush, and the stop mining line is located at the protective coal pillar of the mine industrial square. The 2-2 coal seam is the main seam of LW2215, and the coal seam and its top and bottom floor have a tendency to experience weak rock burst. In addition, it is characterized by an average mining depth of 731.4 m, simple structure, small fluctuation changes, average dip angle of 2° , coal seam thickness ranging 5.64~7.33 m and an average of 6.41 m, simple geological conditions, hidden small faults, and lack of magmatic rock mass, collapse column and other geological structures in the mine field. LW2215 has a width of 300 m and a length of 2709 m, and a strike longwall full-mechanized coal caving method is adopted for mining. The coal pillar between LW2215 tailgate and LW2217 headgate is 5 m, and snf 80 m away from the LW2217 headgate is an LW2217 auxiliary transport roadway, which is connected through 3 connection roadways, where 1 is found in the middle of the working face connecting the headgate and tailgate. By 31 December 2021, the LW2215 had been mined to about 1420 m, as shown in Figure 2. The microseismic monitoring system is SOS, developed in Poland [42]. An amount of 9 microseismic sensors are arranged around LW2215, among which 14#, 15# and 16# are arranged on the surface, and sensors 2#, 4#, 5# and 8# are constantly moved and optimized along with mining on the working face. These sensors are used to monitor mine seismic events in the mining process and capture precursor information regarding rock burst. According to the 6 boreholes on the working face, the distribution of overlying strata in the coal seam is shown in Figure 3. It can be seen that there are multi-layer thick and hard roofs above the coal seam, forming a thick hard roof group structure.

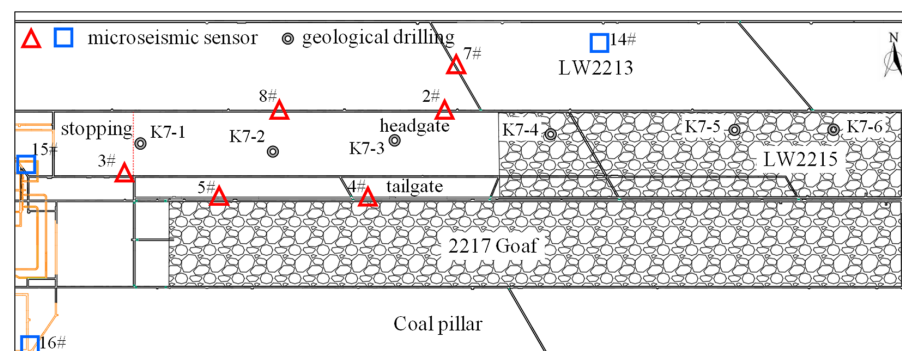


Figure 2. Layout of the LW2215. The circle is geological drilling, the triangle is microseismic sensor arranged on the underground in the mine, and the square is microseismic sensor arranged on the surface.

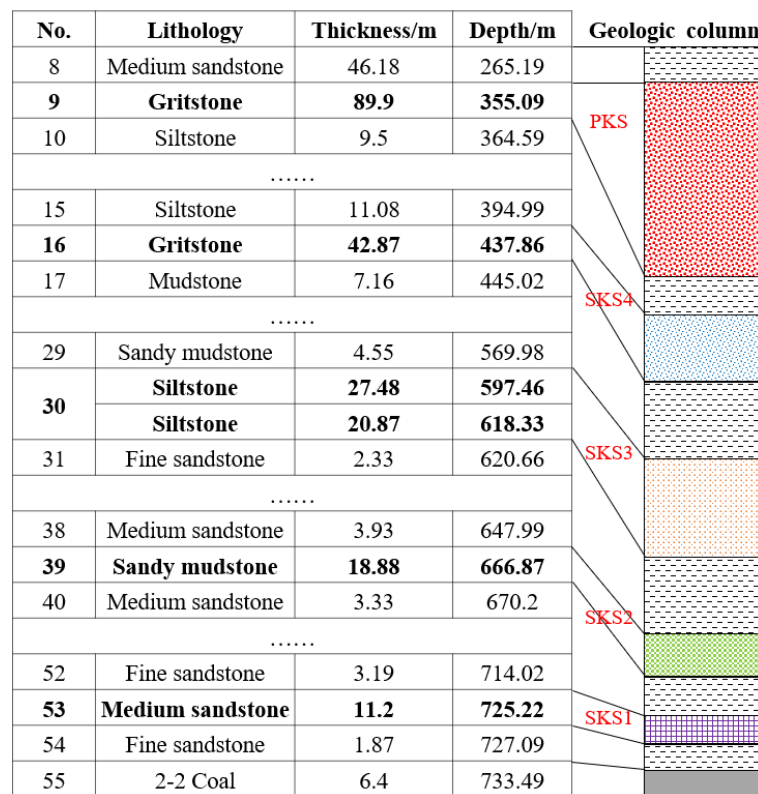


Figure 3. Formation structure of the LW2215. Different colors represent different lithologies.

The key strata theory proposed by Qian [43] is focused on mining-caused rock strata movement, with an in-depth study of the rock strata movement from the basic roof to the primary key strata (PKS), which provided strong support for revealing the mechanism of mine seismicity and rock burst induced by the overburden fracture movement. For the working face with a multi-layer thick and hard roof above, the key strata should first be identified. The bearing capacity of the multi-layer thick and hard roof composite structure meets the following requirement [44]:

$$q_1(x)|_m = E_1 h_1^3 \sum_{i=1}^m h_i \gamma_i / \sum_{i=1}^m E_i h_i^3 \tag{1}$$

where $q_1(x)|_m$ is the load formed by strata m on the first hard strata, h_i is the thickness of strata i , γ_i is the rock bulk density of strata i , E_i is the elastic modulus of strata i and $i = 1, 2, \dots, m$.

The load formed by the strata $m + 1$ on the hard rock strata 1 is:

$$q_1(x)|_{m+1} = E_1 h_1^3 \sum_{i=1}^{m+1} h_i \gamma_i / \sum_{i=1}^{m+1} E_i h_i^3 \tag{2}$$

The strata m is determined to be the key strata if it satisfies the following requirement:

$$q_1(x)|_{m+1} < q_1(x)|_m \tag{3}$$

Substituting Equations (1) and (2) into Equations (3) and simplifying them, we obtain:

$$E_{m+1} h_{m+1}^2 \sum_{i=1}^m h_i \gamma_i > \gamma_{m+1} \sum_{i=1}^m E_i h_i^3 \tag{4}$$

The position of hard rock strata in overburden rock and the soft rock strata group are obtained by discriminating the position of hard rock strata. No.16 gritstone, No.30 siltstone, No.38 sandy mudstone and No.53 medium sandstone are identified as the subordinate key strata (SKS), and No.9 gritstone as the PKS, as shown in Figure 3.

2.2. Description of Large-Energy Mine Seismic Events on the Working Face

Since January 2022, the warning index of microseismic events had been reduced from 5.0×10^5 J to 8.0×10^4 J for single-event energy. By 31 May 2022, 52 EWI mine seismic events had occurred on the LW2215. Of these, 40 events were located in front of the working face, accounting for 76.90%, and 12 were in the goaf behind the working face. The plane projection for mine seismic events is shown in Figure 4, and detailed statistics are in Table 1. In Figure 4, the purple area indicates the scope of mining from 1 January to 31 May 2022, and the red and yellow circles the EWI mine seismic events.

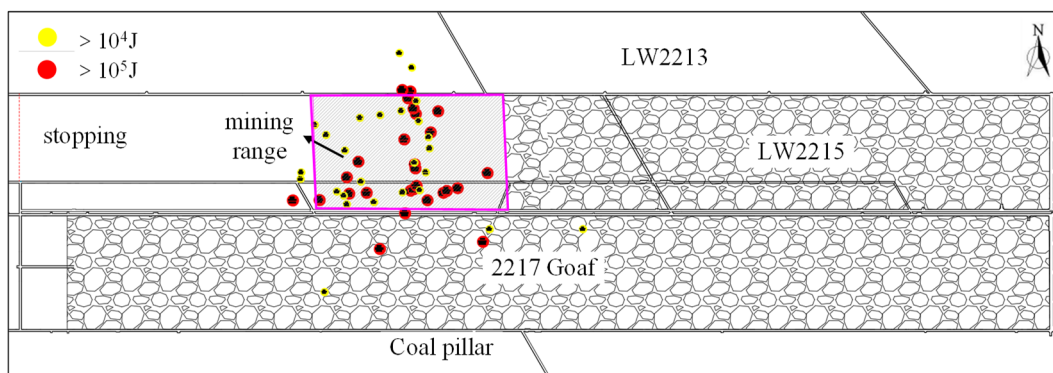


Figure 4. Plane projection of EWI mine seismic events in LW2215. The purple box indicates the scope of mining from 1 January to 31 May 2022.

Table 1. Analysis of EWI mine seismic events in LW2215.

Location		Number of Events per Month				
Working Face Ahead	Behind the Working Face	January	February	March	April	May
40	12	4	12	24	6	6
Footage per month/m		111.6	99.6	104.8	104.4	90.4

According to the statistical data, 36 EWI mine seismic events occurred mainly in February and March. Typical mine seismic events are described as follows:

(1) The EWI mine seismic events occurred in front of the working face: on 16 January 2022, a 3.31×10^5 J energy-level event occurred, which was located 88 m in front of LW2215. The floor heave within the range of 40–50 m in front of the working face increased by 100–150 mm, and the displacement of the roadway’s side within the range of 50–60 m in front of the work increased by about 200 mm. On 14 February 2022, a 3.54×10^5 J energy-level event occurred, 34 m in front of LW2215, accompanied by the phenomenon of coal cannon [45]. On 8 March 2022, a 2.78×10^5 J energy-level mine seismic event occurred, 10 m in front of the working face, accompanied by the phenomenon of coal cannon.

(2) The EWI mine seismic events occurred behind the working face: on 8 February 2022, a 1.58×10^5 J energy-level mine seismic event occurred, located about 38 m behind 2215 working face, accompanied by large sound of coal cannon. On 24 February, a 3.29×10^5 J energy-level mine seismic event occurred 112.2 m behind the working face, accompanied by the loud sound of a coal cannon.

Due to the goaf behind the working face, the occurrence of mine seismicity in the goaf has little influence on the roadway, so this paper mainly studies large-energy mine seismic events in front of the working face.

3. Analysis of Key Factors of Frequent Mine Seismic Events in Goaf Mining

3.1. Analysis of the Overlying Thick and Hard Roof Characteristics

According to Figure 3 in Section 2.1 and the identification of key strata, the rock formation above LW2215 is relatively special. There are 5 groups of key strata above the 2-2 coal seam, among which SKS1 is 11.2 m thick medium sandstone located 1.87 m away from the coal seam. SKS2 is 18.8 m thick sandy mudstone located 60.22 m away from the coal seam; SKS3 is 48.35 m thick siltstone located 108.76 m from the coal seam; SKS4 is 42.87 m thick gritstone located 289.23 m away from the coal seam; PKS is 89.9 m thick gritstone located 372 m away from the coal seam, above which is entirely interbedded sandstone except for 66.2 m thick aeolian sand.

Through exploration of the development height of the water-conducting fracture zone in the overlying rock of LW2217 that has been mined, it can be seen that the development height of the water-conducting fracture zone in the roof of LW2217 is 115.5 m. According to the mining height of 5.5 m, the ratio of mining height and fractured zone height is 21, as shown in Figure 5. After the mining of LW2215, the overlying strata in the goaf will move again, and the height of the fracture zone on the working face will further expand. According to the rock movement theory proposed by Qian [44] and the three-zone structure loading model of overlying strata proposed by Jiang [46], when the gob-side working face is mined to double square, the height of the overburden fracture zone will reach about two times that of the single working face. Therefore, it is estimated that the height of the fracture zone will develop to 210~230 m.

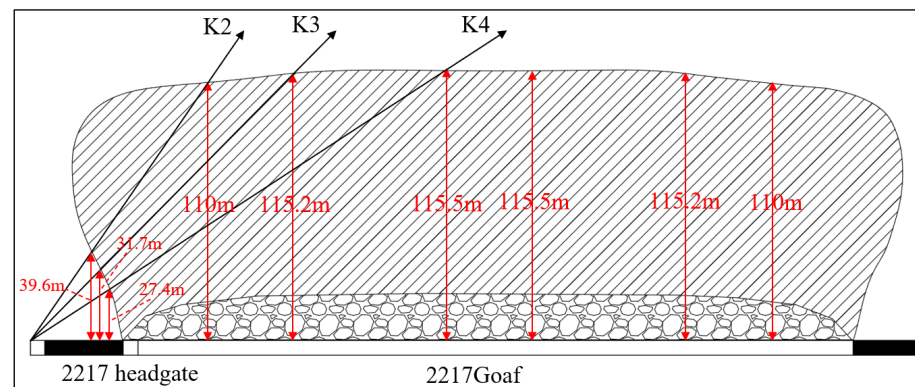


Figure 5. Development height of the water flowing fractured zone of LW2217. The different numbers represent the development height of water-conducting overlying fracture zone at different positions in the goaf.

According to the results for estimating the failure height of the three overlying zones combined with overlying key strata, it can be concluded that:

(1) SKS1, SKS2 and SKS3 of LW2215 working face are located 0~150 m above the coal seam. Therefore, it can be inferred that SKS1, SKS2 and SKS3 are located in the control area of the fractured zone of the working face during the mining of LW2215, and the broken part is used as a caving zone to fill the goaf. They mainly control the movement and deformation of rock strata in the caving and fracture zones.

(2) SKS4 and the main key strata of LW2215 are interbedded sandstone groups with thick layers located more than 280 m away from the coal seam and above the fracture zone, which mainly controls the bending and subsidence of the roof structure. At the same time, due to the increased thickness from the combination of rock, strong integrity, and the fact that the subsidence between the lower rock is not synchronous, it is easy to

separate between the strata and the lower rock, forming a suspended plate structure, and the distance from the ground is close, so the breaking instability easily affects the surface, and the ground produces co-seismic activity, forming the basis for a large-energy mine seismic event.

3.2. Analysis of Surface Subsidence

Deep mining can cause surface subsidence and even lead to secondary disasters such as large-scale collapse [47,48]. Therefore, a number of surface rock movement monitoring lines are arranged in mining area 22 to regularly monitor surface subsidence in the mining process of the working face. The layout of measuring lines is shown in Figure 6.

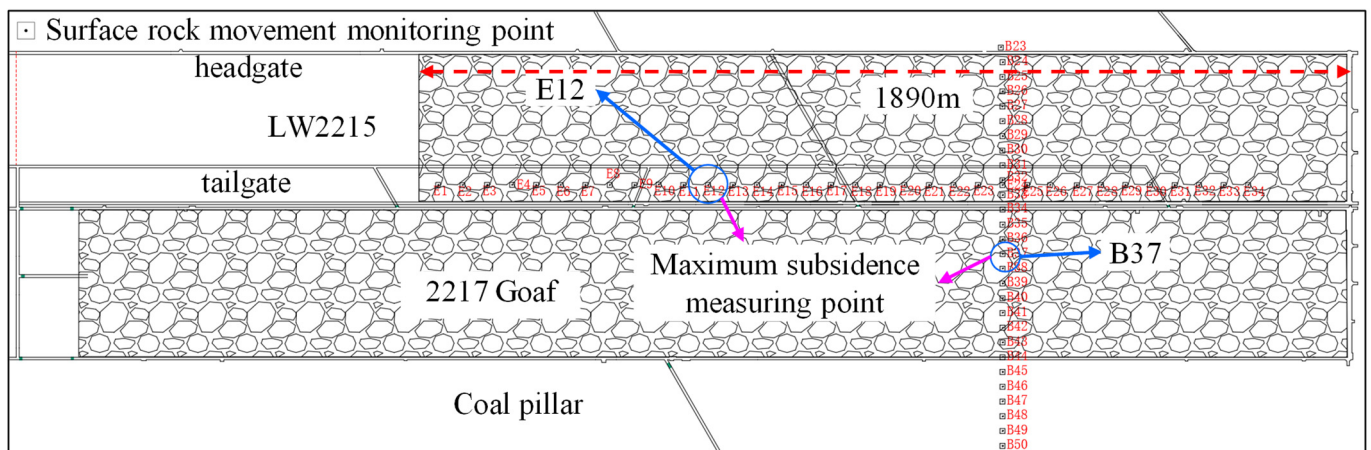


Figure 6. Surface rock movement monitoring point layout diagram of LW2215. The different numbers represent the different surface displacement measurement points.

As of June 2022, the latest date for surface subsidence data monitoring is 15 May 2022, based on which the surface subsidence in the mining process of LW2215 is analyzed. The LW2215 started mining in August 2019, and by 15 May 2022, the LW2215 had mined about 1890 m. At this time, there was a tendency for the maximum subsidence point to be at B37, and the maximum subsidence point on the strike was E12. The measuring point of the maximum subsidence points are marked in Figure 6.

The measuring point B37 is located in goaf 2217, in the square area of the double working face. The accumulated subsidence is 1680 mm, and the subsidence rate is only 26.2%, indicating that there was tendency not to reach full subsidence. The subsidence of a similar position in goaf 2215 is far less than that in goaf 2217. This indicates that the overlying strata caving in goaf 2215 is still insufficient compared with goaf 2217 (as shown in Figure 7a). The measuring point E12 is located in goaf 2215, and the subsidence basin formed by the goaf strike of LW2217 and LW2215 does not have a “flat bottom” [47] (as shown in Figure 7b). The accumulated subsidence is 1270 mm, and the subsidence rate is only 19.8%, indicating that full subsidence has not been reached in the goaf strike. In summary, the surface subsidence has not reached a full settlement state in terms of strike and trend, and with the continuous progress in the working face, the surface subsidence has not changed significantly, indicating that at this time, the formation activities have stabilized. According to the key strata theory proposed by Qian [43], the key strata control the activity of the overlying strata. Combined with the observation results of surface subsidence on the strike and tendency of LW2215, it can be seen that when the working face advances through the square of the double working face, the maximum subsidence tends to increase by 410 mm compared with the maximum subsidence on the strike, indicating that with the mining of the LW2215, the fracture height gradually expands upward. At this time, SKS4 fracture occurs, and the PKS may be separated and in the stage of bending

subsidence. It is confirmed that the middle and high key strata will gradually fracture with expansion of the mining scope, triggering more mine seismic events.

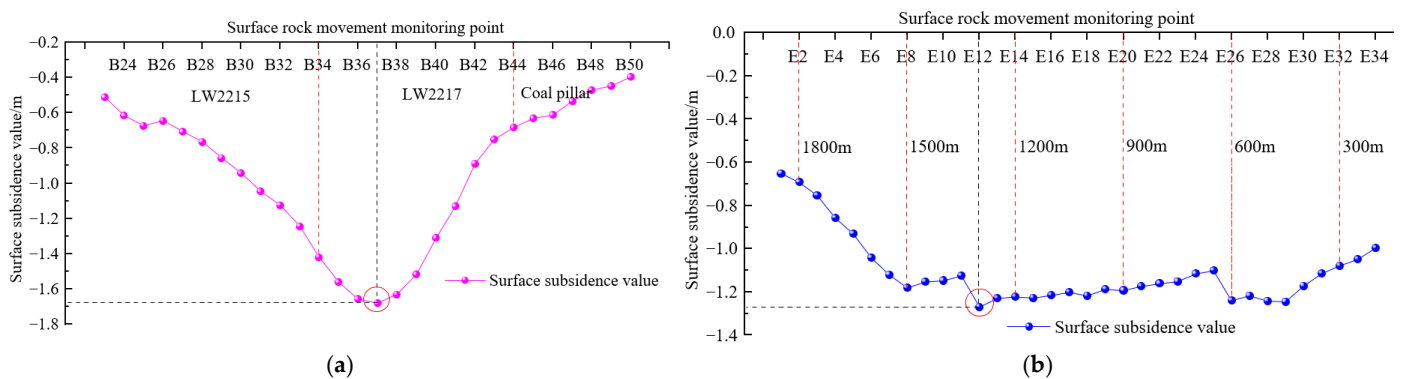


Figure 7. Surface subsidence curves of LW2215: (a) surface subsidence curve in the direction of tendency; (b) surface subsidence curve in the strike direction.

3.3. Determination of Overlying Rock Spatial Structure

The appearance of ground pressure in the working face is closely related to the structure morphology and movement characteristics of mining-induced rock strata, while the microseismic events in the working face reflect the rock macro fracture behavior of the rupture and fracture connection of the mining rock strata [49]. The density and accumulation (space domain) and frequency of occurrence (time domain) of microseismic signals are factors in the frequent occurrence of rock fracture and rupture in this area. LW2215, as the first working face along the goaf, is fractured along the mining strata, and its structural form during its mining process is shown in Figure 8a. SKS1 enters the caving zone to form a cantilever beam structure, while SKS2, SKS3 and SKS4 are located in the fracture zone to form a masonry beam structure. In most existing studies [50–52], it is believed that the peak position of advanced abutment pressure on the working face corresponds to the position of advanced fracture in the rock layer. Therefore, according to the outward expansion curve characteristics of the mining stress boundary [46], it can be preliminarily inferred that the key mining strata in LW2215 presents the phenomenon of advanced fracture, which is consistent with the phenomenon that most mine seismic signals concentrate in front of the working face. As shown in Figure 8, according to the thickness of each key strata and its relative distance from the coal seam, the fracture characteristics of the key strata and the location and morphology of initiation fissure can be inferred. For the PKS, there should be no macroscopic fracture, nor obvious formation of masonry beam structure, but the thickness of the PKS is large, affected by the central bending and deflection, the central span of the key strata should appear as local fracture and rock stripping, and the overall subsidence is not substantial.

From the perspective of the three-dimensional shape of the mining rock structure, in the mining process of LW2217, the lower subordinate key strata of the roof, such as SKS1, breaks to form the cantilever beam structure and enters the caving zone. The middle subordinate key strata, such as SKS2 and SKS3, are in the crack zone. According to the “O-X” fracture characteristics of the plate structure [53], the articulation form of the masonry beam structure can be drawn along its direction, together with the breaking law of the plate structure. When the mining of LW2217 is finished, the upper key strata on the working face has not yet been broken. A lateral fault line is formed at the critical point between the middle and lower key strata above the goaf of LW2217 and LW2215. In Figure 8b, this fault line leads to the existence of a side hanging plate on the goaf side throughout the entire duration in which there is mining of LW2215.

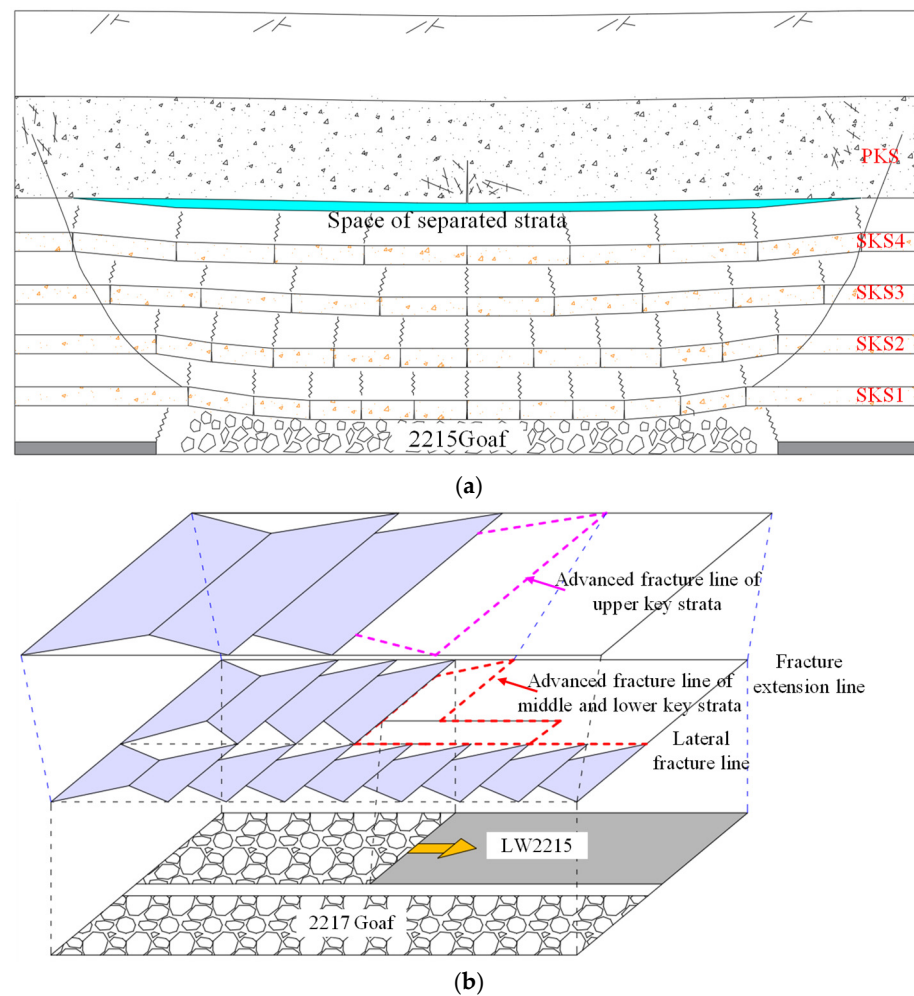


Figure 8. The fracture structure of the thick and hard roof group in LW2215 during the mining process: (a) fracture structure morphology; (b) high L-shaped roof structure diagram and its advanced fracture characteristics.

When mining began in LW2215, accompanied by the advance of the working face, the roof above the low SKS gradually becomes broken, according to the “O-X” type of breaking, to form the hinged block of masonry beam structure in the early stage of LW2215 mining. Although mining is double-sided, the upper key strata still have not been broken due to the small mining space or relatively small mining range. When cumulative mining of the LW2215 working face reaches a certain distance, the top plate of high key strata breaks for the first time and then enters into a cycle of breaking. At this time, due to the lateral suspension plate formed by the fracture of the lower SKS in the LW2217 above the LW2215 and the coupling influence of the roof of the LW2215, an L-form “advance and lateral” roof is formed in the process of mining LW2215, as shown in Figure 8b. According to the key strata theory of rock strata control, the fracture step of the upper key strata must be greater than that of the lower key strata. At this time, if only the L-form composite roof of the middle key strata is broken during the advancing process of LW2215 while the upper key strata remain unbroken, then the pressure development and mine seismic energy events of LW2215 mining may be relatively small. However, if the L-form composite roof of the SKS in the middle of the activation coincides with periodic fracture of the high key strata, the combined effect of the two will lead to the frequent occurrence of large-energy mine seismic events in LW2215, the location of which are mostly in front of the working face.

Figure 9 shows the fracture structure morphology of the thick and hard roof group in the mining process of the working face, in which the width of a single working face is 300 m, and there are 5 key strata overlying the coal seam. Under the condition of single

mining, the maximum height of the fractured rock formation structure above the stope is about 150 m, or half of the width of the short side of the mining range [47].

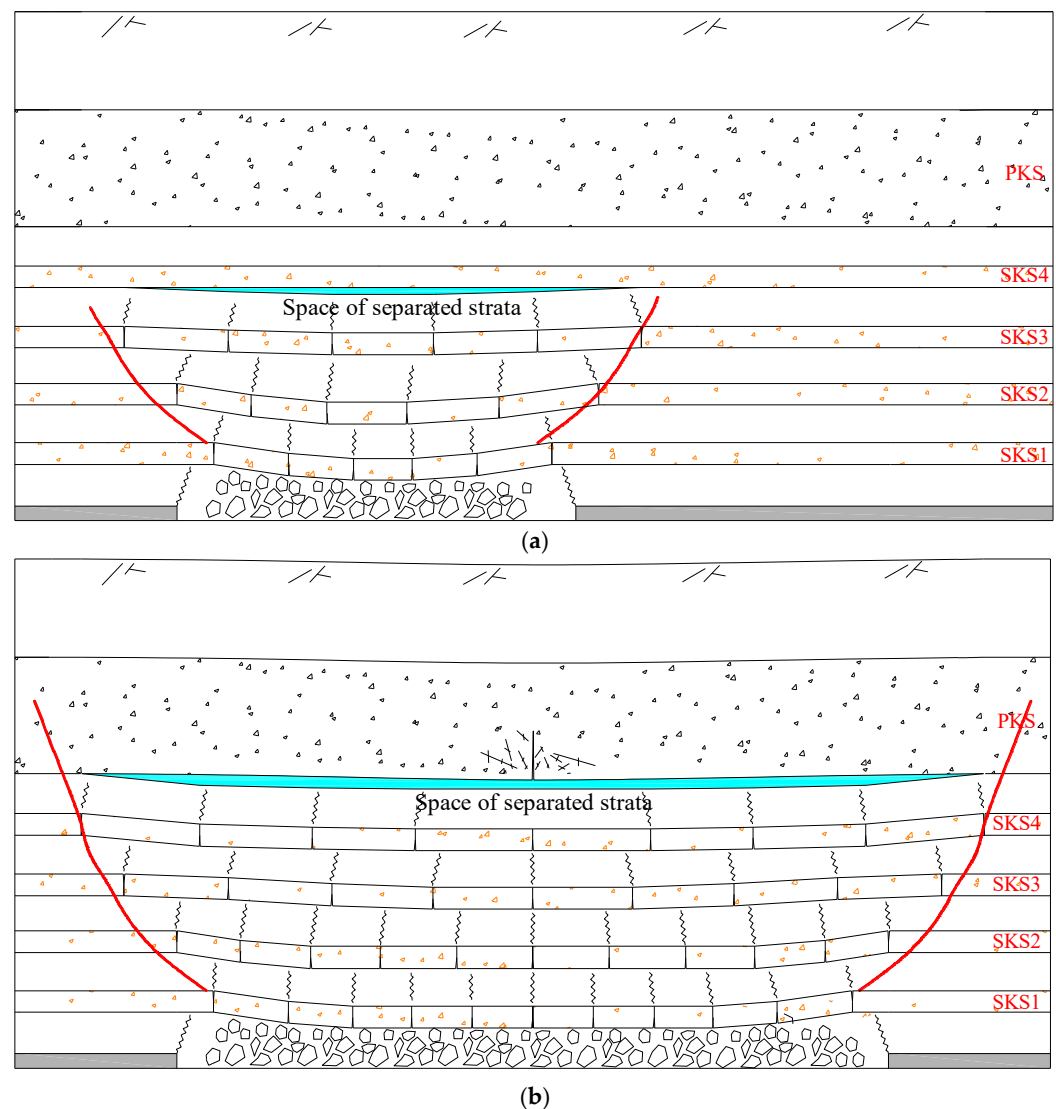


Figure 9. Fracture structure morphology tendency of the thick and hard roof group: (a) single-working-face mining; (b) double-working-face mining.

At this time, separation of the SKS1~SKS3 rock formation fracture and KS4 strata occurs. When the second working face is mined, especially when the working face is pushed to the square of the double working face, the fracture height gradually expands upward, and the maximum height can reach 300 m. At this time, the fracture of SKS4 occurs, and the separation of the PKS may occur. This also indirectly confirms that under the double-sided mining strip, the middle and high key strata will gradually break along with the expansion of mining scope. Simultaneous breakage of the high, middle and low SKS will trigger more large-energy mine seismic events as a result of the superposition effect.

3.4. Field Verification of Thick Hard Roof Group Structure

Each mine seismic event has rich temporal and spatial information [54]. Real-time monitoring and processing of mine seismic events can be used to identify the occurrence location and intensity of mine seismic events, further determining the stress transition inside a coal rock mass. From 1 January to 31 May 2022, a total of 52 EWI mine seismic

events occurred in LW2215. In order to better grasp the law of advance distribution of mine seismic events, the distribution of mine seismic events over 10^4 J in each month was analyzed, and the monthly plane projection is shown in Figure 10.

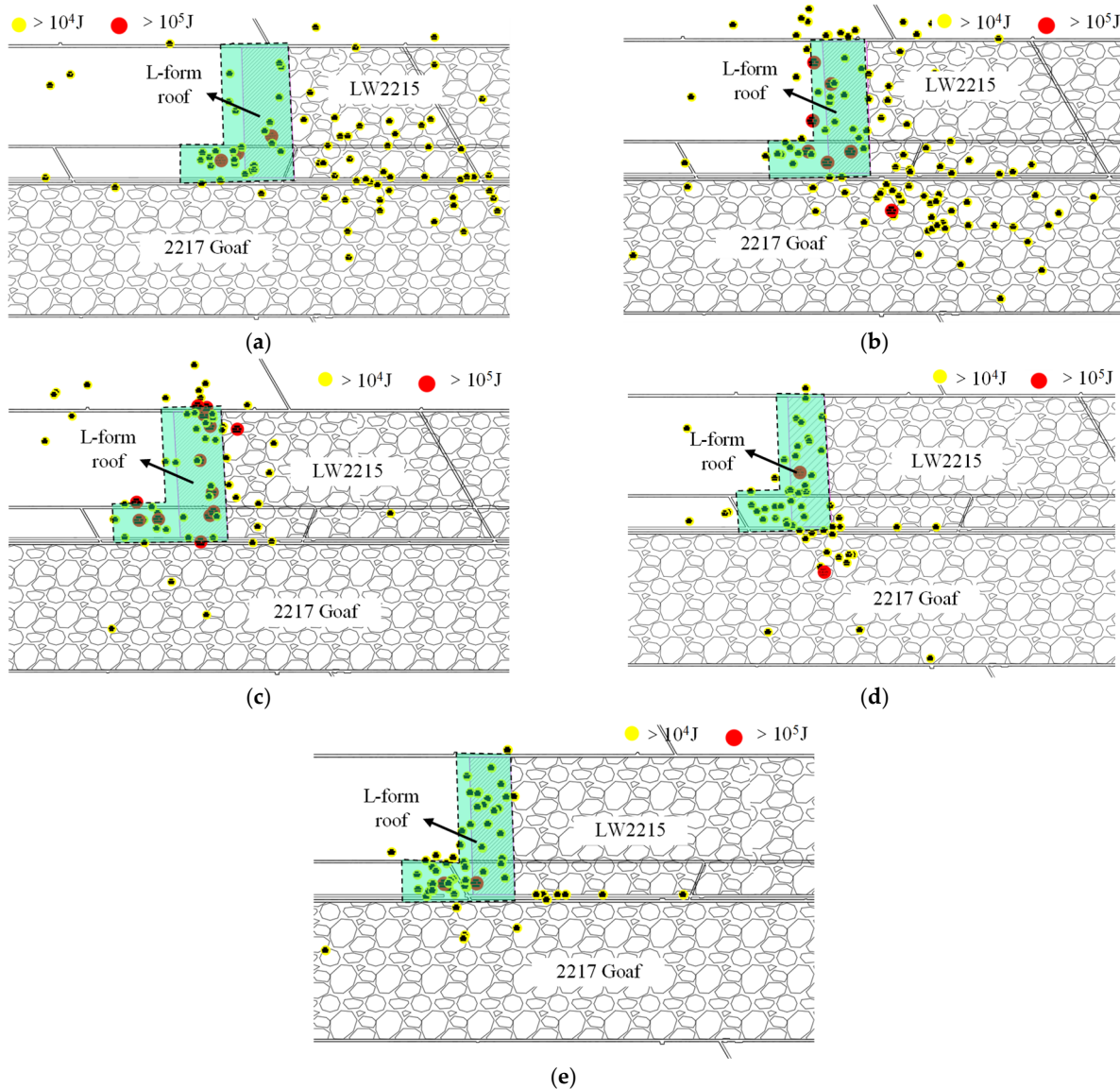


Figure 10. Plane projection of mine seismic events from January to May: (a) January; (b) February; (c) March; (d) April; (e) May.

The mine seismic events and rock burst sources were found mainly located in the main area where the suspended roof and inter-strata rock column are supported by the coal body. According to the above analysis of the surface subsidence, the mining area of LW2215 has not reached full subsidence both in strike and tendency, and there must be a group of thick and hard rock strata or multiple groups of thick and hard rock strata bending deformation. After separation, most of the stress is applied to the coal body in the advanced support area of the working face, forming a fulcrum similar to a “lever” at the coal wall of the working face. As a result, the coal body and the roof at a certain distance ahead of the horizontal stage produce stress concentration and accumulate a large amount of elastic deformation energy. When the accumulated energy reaches a certain degree, the coal rock mass is internally fractured, and mine seismicity occurs. It is revealed that there is a high correlation between large-energy mine seismic events and the bending and prying effect of the thick hard roof group.

At the same time, it can be found that there are mine seismic events of energy higher than 10^5 J in the headgate, tailgate and the front of the working face. The ore seismic events in the tailgate near the goaf 2217 are more concentrated, and most of the events are distributed between 40 m and 120 m ahead of the working face. The area where mine seismic events are concentrated shows an obvious L-form distribution in the leading and goaf side of the working face, as shown in the green area in Figure 10. At this time, it is confirmed that the roof is affected by the coupling of lateral suspension plate and advance suspension plate, forming an L-form roof that is “advance and lateral” in space.

3.5. Impact Analysis of Mining Speed

The corresponding relationship between daily footage and microseismic event statistics during mining in LW2215 from 1 January to 31 May is analyzed, as shown in Figure 11. The green arrow in Figure 11 indicates a day in which there was occurrence of a mine seismic event of more than 10^5 J energy. As can be seen from Figure 11a, the mining speed in January is relatively stable, mostly 4 m/d, and the mining speed was 4 m/d for the 3 mine seismic events exceeding 10^5 J. The total daily energy of microseismic events was low in the days before the occurrence, and the rock strata accumulated a lot of energy, which was not fully released and led to occurrence of the three events. This indicates that the EWI event in January has no significant correlation with the mining speed.

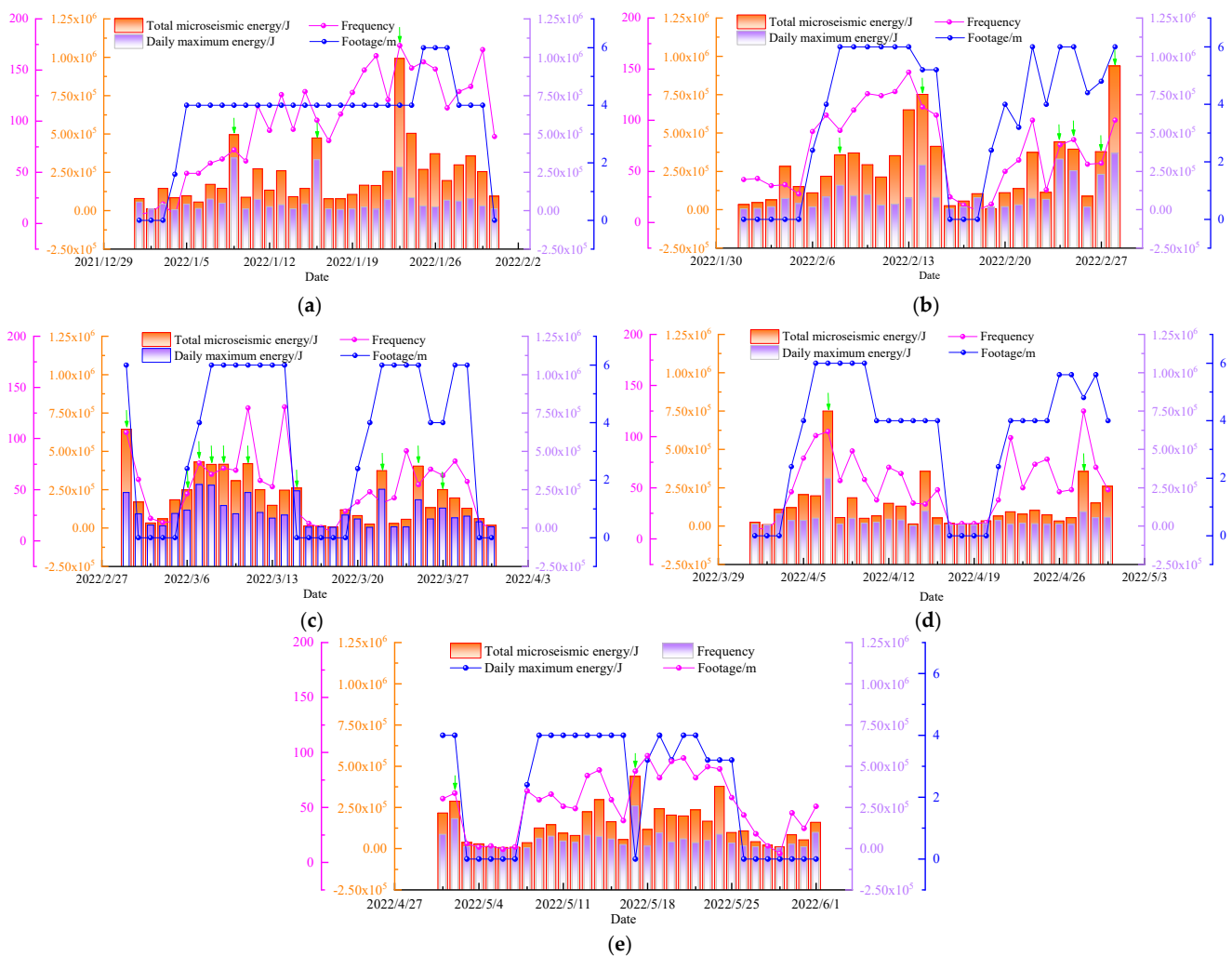


Figure 11. Curves of daily advance and microseismic energy from January to May; the frequency is number of events per day: (a) January; (b) February; (c) March; (d) April; (e) May. The green arrows represent EWI mine seismic events that occurred that day.

According to Figure 11b–e, microseismic energy and frequency are positively correlated with the mining speed from February to May. When the mining speed increases to 6 m/d, the microseismic energy and frequency increase significantly. In addition, the recent large-energy mine seismic events on the working face all correspond to the stages of relatively high mining speed (6 m/d), sudden increase (0–6 m/d) and sudden drop (6 m/d-0). With the increase in mining speed, the surrounding rock stress adjustment time is shortened, the direct roof caving is insufficient, the coal rock mass easily accumulates energy and the working resistance of the support on the working face is increased. With the continuous mining of the working face, the coal rock formation breaks in front of and behind the working face, inducing large-energy events. When the mining speed is reduced to below 4.8 m/d, there are significant reductions in over-limit events. Therefore, the degree of microseismic activity during mining of LW2215 is closely related to the change in mining speed, which is one of the main reasons influencing the number of EWI mine seismic events.

In summary, the main reasons for the number of EWI mine seismic events in LW2215 and their location in the leading section of the working face are induction of an L-form “advance and lateral” roof, gradual breaking of the multi-layer thick and hard roof, the bending and prying effect of the thick hard roof group, and excessively fast or uneven mining speed.

4. Measures for Prevention and Control of Large-Energy Mine Seismic Events during Subsequent Mining on the Working Face

4.1. Controlling the Mining Speed

The main source of large-energy mine seismic events and induced disasters are the deformation of key strata [14]. Studies have shown that regardless of the cantilever beam structure in the key strata in caving or the low masonry beam structure in the fracture zone, under the same mining time and with the increase in mining speed, the more elastic energy that accumulates in the coal mass before the hard roof fracture, the greater the energy of mine seismic events [51]. However, considering the economic benefits and safe production, there must be a critical mining speed for the working face such that the energy released by the movement of the hard roof can be kept at an appropriate level, i.e., not high enough to induce mine seismic and rock burst.

Therefore, the key to mine seismic event prevention and disaster reduction is to control the length of the overhanging roof and coordinate the relationship between the overhanging roof length and the stress release rate while keeping the surrounding rock in a state of “low stress, low density, low disturbance and strong support” [55]. In order to better analyze microseismic response characteristics under different mining speeds, 52 mine seismic events with a single energy at least 8.0×10^4 J from 1 January to 31 May 2022, are selected for analysis. The daily footage is set as 4.4 m, 4.8 m, 5.6 m and 6.4 m. When the daily footage is less than the set value, the frequency and proportion of mine seismic events are separately counted, as shown in Table 2 and Figure 12.

Table 2. Daily footage corresponds to the number of mine seismic events.

Daily Footage/m	4.0	4.8	5.6	6.4
Times	24	26	28	52
Proportion/%	46.15	50.00	53.85	100

It can be seen that there is a positive correlation between daily footage and the frequency and proportion of large-energy events. Specifically, when the daily footage is less than 4.0 m, the proportion is only 46.15% of all large-energy events. The frequency increases by 2 and 4 when the daily footage is 4.8 m and 5.6 m compared with when it is 4.4 m, accounting for 3.85% and 7.7%. When the daily footage increases to 6.4 m, the frequency and proportion increases sharply, by 24 and 46.15% compared with at 5.6 m. According to the above analysis, the daily footage of 5.6 m is a turning point in the process of advancing

the working face. When it exceeds 5.6 m, the frequency and proportion increase significantly; when it is less than 5.6 m, although the frequency and proportion both increase with the increase in daily footage, the amplitude is small. Considering the safety factor, it is suggested to maintain the mining speed at less than 4.8 m/d in the process of further mining on LW2215. When special geological areas such as hidden faults and folds are encountered, the maximum mining speed should not exceed 4 m/d, and the mining speed should be kept as uniform as possible.

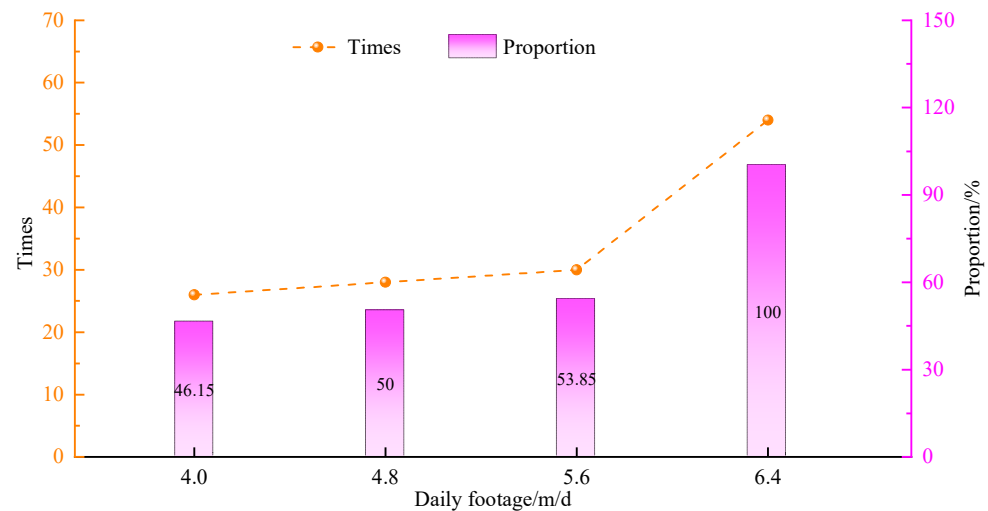


Figure 12. Daily footage corresponds to the proportion of mine seismic events.

4.2. Strengthening Measures of Blasting Roof Breaking on the Working Face

The vertical depth of the underground roof blasting boreholes is generally not more than 100 m [40]; beyond 100 m, it is difficult to meet the construction requirements for the drilling machine, charging and sealing. According to the column chart of drilling in LW2215 working face (Figure 3), the range of drilling and blasting in the roof mainly includes two strata, namely SKS1, 1.87 m away from the coal seam, and SKS2, 60.22 m away from the coal seam. The blasting roof breaking boreholes in the two roadways of the LW2215 are optimized. The inclined boreholes are arranged in high, medium and low positions, and the strike boreholes are arranged in high positions. The inclined boreholes of the tailgate are arranged in combination with the strike boreholes in the same section to promote the roof breaking effect. The advance distance of headgate is not less than 300 m, and the tailgate is not less than 350 m, as shown in Figure 13.

(1) Inclined boreholes of tailgate: construct a group of high, medium and low boreholes in the inclination of diameter $\Phi 80\sim 89$ mm and 15 m spacing. For high boreholes, the depth is 80 m, angle is 65° and charging is 20 m. For medium boreholes, the depth is 42 m, angle is 55° and charge is 15 m. For low boreholes, the depth is 30 m, angle is 45° and charging is 12 m, as shown in Figure 13b. The azimuth vertical roadway toward the working face construction, high, medium and low boreholes have a spacing of 100–200 mm in the side shoulder socket near the position, with a charging decoupling coefficient not greater than 1.3.

(2) Strike boreholes of tailgate: For construction strike boreholes, the diameter is $\Phi 80\sim 89$ mm, spacing is 15 m, borehole depth is 80 m, angle is 65° and charging is 25 m, as shown in Figure 13c. For the azimuth parallel roadway toward the goaf construction, the charging decoupling coefficient is not greater than 1.3, and the tailgate blasting roof breaking form “4 + 1 + 4” blasting effect. The “4 + 1 + 4” blasting effect refers to the “4 boreholes + 1 borehole + 4 boreholes” in the direction of the working face in the tailgate.

(3) The parameters of the blasting boreholes of the headgate are consistent with those of the tailgate on the LW2215.

The blasting roof breaking within the working face is carried out every 100 m along the strike direction. Four groups of blasting boreholes are arranged on the working face, with a group spacing of 60 m, and 2 boreholes are arranged in each group. The spacing of boreholes in the group is not less than 2 m, the diameter is $\Phi 80\sim 89$ mm, the high boreholes depth is 80 m, the angle is 65° , the charge is 25 m; the low boreholes depth is 65 m and the angle is $65^\circ (\pm 5^\circ)$, as shown in Figure 14.

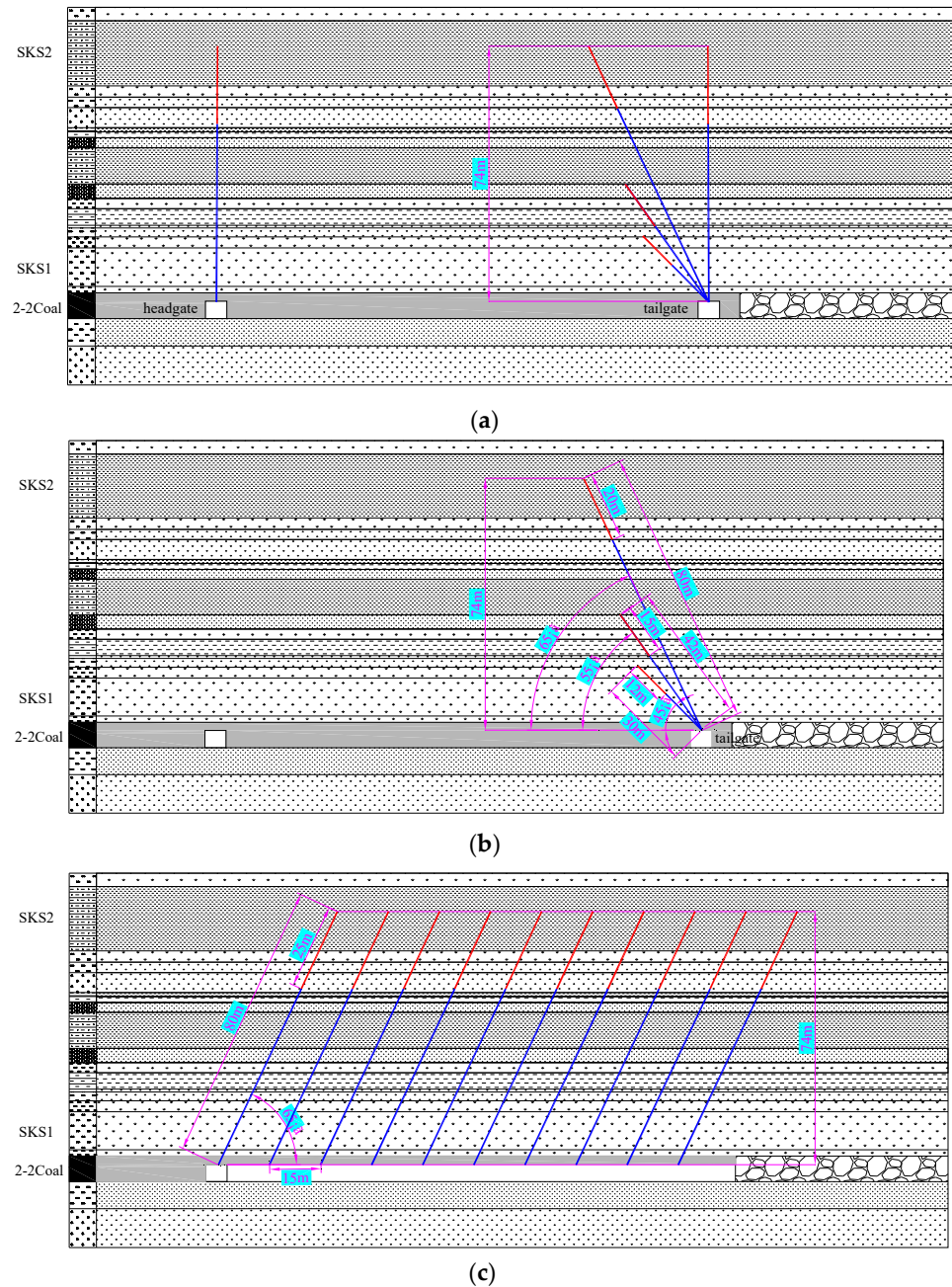


Figure 13. Two roadways roof blasting boreholes layout scheme of LW2215: (a) profile design of roof presplitting boreholes of two roadways; (b) profile design of inclined roof presplitting boreholes of tailgate; (c) profile design of strike roof presplitting boreholes of two roadways. Red is the boreholes charging section, blue is the borehole sealing section.

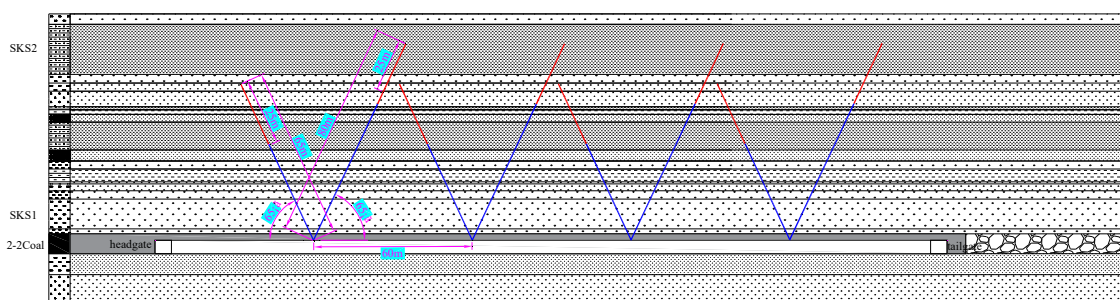


Figure 14. Layout of roof blasting boreholes within the LW2215. Red is the boreholes charging section, blue is the borehole sealing section.

4.3. Effect Test

In February and March 2022, there was an excess of EWI mine seismic events. Therefore, mining was temporarily stopped on 30 March, and the measure of blasting roof breaking was taken along 2 roadways and within the working face. By the end of May, 2 rounds of blasting within the working face had been completed, with a total of 16 blasting boreholes within the working face and 100 roof-blasting boreholes in 2 roadways construction. The data for the 2 months before and after the blasting of the roof were selected for analysis, in which the cumulative advance of the working face was 204.4 m in February and March, and 194.8 m in April and May, as shown in Table 3 and Figure 15.

Table 3. Statistical table of microseismic events before and after blasting.

Energy Classification	Changes in Energy and Frequency of Microseismic Events with Different Energy Levels before and after Blasting					
	Total Times			Total Energy		
	Before Blasting	After Blasting	Proportion of Increase	Before Blasting	After Blasting	Proportion of Increase
$10^2 \sim 10^3$ J	2498	3279	31.27%	9.01×10^5	1.15×10^6	27.64%
$10^3 \sim 10^4$ J	982	1046	6.52%	2.87×10^6	3.23×10^6	12.54%
$10^4 \sim 10^5$ J	167	172	2.99%	5.74×10^6	6.08×10^6	5.92%
$10^5 \sim 10^6$ J	20	4	−80.00%	4.33×10^6	1.13×10^6	−73.90%

According to Table 3 and Figure 15, when the mining time is the same for 2 months and the footage is similar, the frequency and total energy of microseismic events at all levels change to differing degrees after the implementation of blasting roof breaking. Among them, the number of $10^2 \sim 10^3$ J microseismic events increased by 781, corresponding to an increase rate of 31.27%, and the increase rate of total microseismic energy is 27.64%. The number of 10^3 J~ 10^4 J microseismic events increased by 64, corresponding to an increase rate of 6.52%, and the increase rate of total microseismic energy is 12.54%. The number of 10^4 J~ 10^5 J microseismic events increased by 5, corresponding to an increase rate of 2.99%, and the increase rate of total microseismic energy is 5.92%. The number of microseismic events greater than 10^5 J decreased significantly from 20 to 4, corresponding to a decrease rate of 80.00%, and the decrease rate of total microseismic energy is 73.9%. The results show that after blasting roof breaking on the working face, the low-energy microseismic events can be increased and the high-level microseismic events can be reduced to a certain extent, which indicates that blasting roof breaking is effective at the source, and the vibration energy transmitted to the working face is very small.

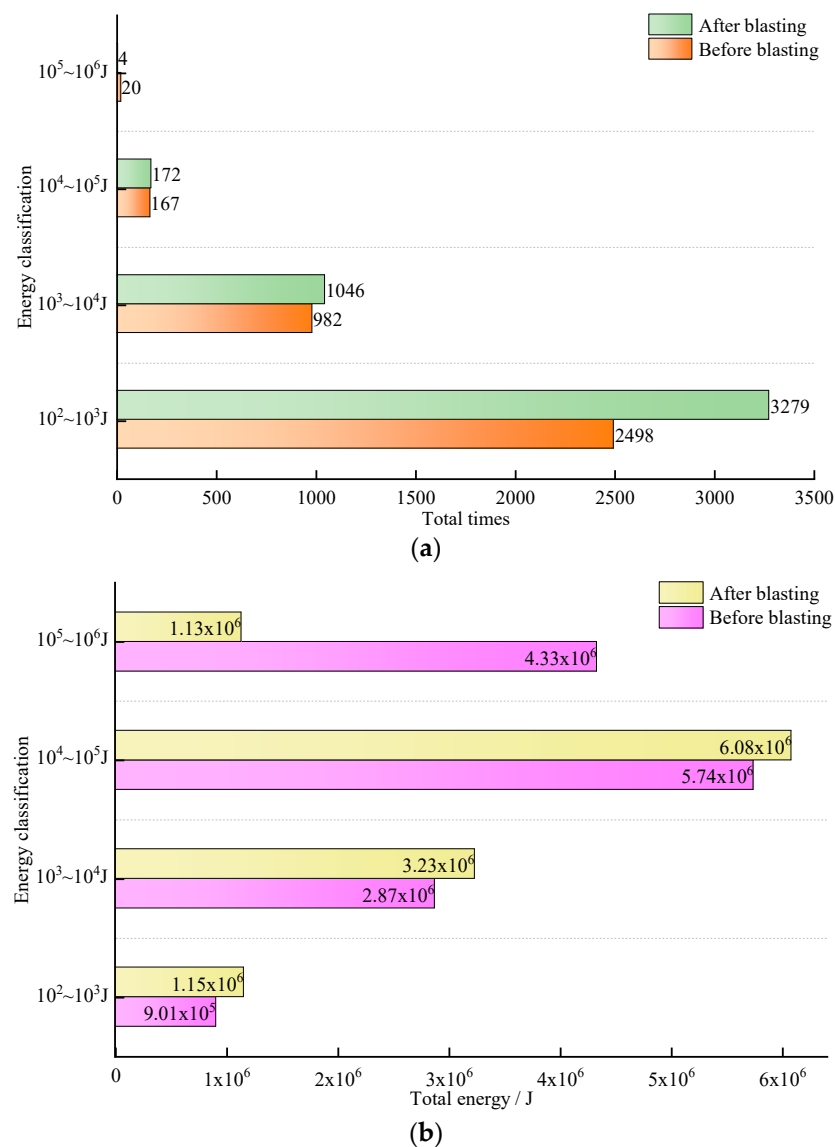


Figure 15. Comparison of microseismic events before and after blasting: (a) total energy; (b) total frequency.

At the same time, as can be seen from Figure 10d,e above, since April, the mining speed of the working face is lower—at 4 m/d most of the time—and the total energy and times of microseismic events have significantly decreased. By controlling the mining speed of the working face and taking blasting roof breaking measures, effective mine seismic reduction and disaster prevention has been achieved.

5. Suggestions and Discussions

In the process of breaking or sliding of thick hard roof, a high amount of elastic energy is suddenly released, resulting in strong vibration, strong dynamic load and high concentrated stress superposition, easily leading to roof and coal seam type (impact pressure type) rock burst or roof type (impact type) rock burst. The thicker the hard rock, the less likely it is to fall, the longer the length of the suspended roof, the larger the area of the suspended exposure for accumulating more elastic energy. In the Ordos mining area of North China, multiple groups of thick hard-bedded sandstone formations commonly exist in the overlying strata of Jurassic coal seams. In recent years, frequent mine seismic events in many large mines of Ordos have resulted in suspended or limited production,

which seriously threatens the safe and efficient operation of 10-million-ton modern mines in China.

The coal seam of Yingpanhao Mine has high strength, high elastic energy index and multiple groups of overlying thick and hard roofs that accumulate more energy, produce higher-energy-level mine seismic events when breaking, and produce greater impact force when breaking. Therefore, the special geological conditions of the mine favor the production of mine seismic events with higher energy levels. According to the observer description of the dynamic phenomenon and the statistics of the mine seismic data, when the energy of the mine seismic event is less than 3.0×10^5 J (see Section 2.2 above for details), there will be no impact on the ground and the underground site, no sense of earthquake on the ground, no damage to the buildings (structures), personnel and property and all work proceeds as normal. Considering the safety factor, it is suggested that the early warning index be set as a single event energy of 2.5×10^5 J and adjusted in a timely manner according to the treatment effect on mine seismic events on the working face.

The existence of multi-layer thick and hard roof overburden strata provides a target for the prevention and control of mine seismic events and induced disasters. Blasting roof breaking in the working face can produce a good fracturing effect on the lower key strata; however, it has limited influence on those mine seismic events induced by the high key strata. At the present stage, field experiments have been gradually carried out in other thick and hard rock mining areas in China, such as isolated grouting for overlying rock [56,57], hydraulic fracturing key strata by surface drilling [31,36,37] and blasting fracturing key strata of ground drilling [55], which have had some effect in mine seismic prevention.

Taking the frequent occurrence of mine seismic events in the mining process of the goaf working face with a multi-layer thick hard roof in Ordos mine as the research background, this study investigates the mechanism and prevention of mine seismic events in the goaf working face. Coordinated blasting to break the roof along two roadways and within the working face is proposed as a measure for preventing and controlling mine seismic events, and an excellent effect on mine seismic reduction and disaster prevention is obtained in field application. The research results can serve as a reference for the development and application of mine seismic mechanism and blasting vibration reduction technology on the working face where there is a multi-layer thick hard roof. Subsequently, according to mine conditions, the appropriate technology should be selected and combined with downhole blasting roof breaking technology to reduce mine seismic events and prevent disasters at the source, so as to ensure the safe and efficient mining of the working face.

6. Conclusions

In view of the frequent occurrence of breaking-type mine seismic events in the goaf working face under the condition of having a multi-layer thick and hard roof, we take a mine in Ordos as the engineering background and adopt the methods of case study, theoretical analysis and field monitoring to investigate the occurrence mechanism and prevention of mine seismic on the goaf working face. The main reasons for the frequent large-energy EWI mine seismic events in LW2215 were revealed, with most events located in the advanced section of the working face. Moreover, coordinated blasting to break the roof along two roadways and within the working face is proposed as a measure for preventing and controlling mine seismic events. The main conclusions are as follows.

- (1) The composition of the strata above the working face is special, comprising multi-layer thick and hard roofs, and the structure of the thick and hard roof group changes after mining. Different roof group structures have different loading mechanisms on the roadway surrounding rock, and the influence areas of the instability dynamic load also differ. When the goaf working face is mined, an “advanced and lateral” L-form roof will form under the coupled influence of the lateral suspension plate formed above the upper working face and the roof of the working face.
- (2) Through the analysis of the multi-layer thick and hard roof structure, surface subsidence and mining speed, it is concluded that the main reasons for the frequent

large-energy EWI mine seismic events in LW2215 with most events located in the advanced section of the working face are induction of an “advanced and lateral” L-form roof, gradually breaking of the multi-layer thick hard roof, the thick hard roof group bending and prying effect, and excessively fast or uneven mining speed.

- (3) Coordinated blasting to break the roof along two roadways and within the working face is proposed as a measure for preventing and controlling mine seismic events, and it was also applied into the field. When the mining time is the same for 2 months and the footage is similar, the frequency and total energy of microseismic events at all levels change to differing degrees after the implementation of blasting roof breaking, resulting in an increase in low-level microseismic events, and high-level microseismic events can be reduced to a certain extent. The frequency of microseismic events greater than 10^5 J is remarkably reduced from 20 to 4 with a decrease rate of 80%, and the rate of decline in total microseismic energy reaches 73.9%, all of which demonstrate the excellent effect on mine seismic reduction and disaster prevention.

Author Contributions: Conceptualization, B.W. and G.F.; methodology, S.Z. and J.B.; formal analysis, B.W. and Z.L.; investigation, G.F. and W.W.; resources, S.Z., Z.G. and J.M.; writing—original draft preparation, B.W.; writing—review and editing, B.W. and J.B.; funding acquisition, B.W. and G.F. All authors have read and agreed to the published version of the manuscript.

Funding: This research was funded by the National Natural Science Foundation of China, grant numbers are No. 52204107 and No. U22A20169, the Distinguished Youth Funds of National Natural Science Foundation of China grant number is No. 51925402; the Fundamental Research Program of Shanxi Province grant number is No. 202103021223072, and the Tencent Foundation or Xplorer Prize.

Data Availability Statement: The data involved in this paper are all included in the text of the manuscript.

Acknowledgments: The authors gratefully acknowledge financial support from the National Natural Science Foundation of China (Grant No. 52204107, U22A20169), the Distinguished Youth Funds of National Natural Science Foundation of China (Grant No. 51925402), the Fundamental Research Program of Shanxi Province (Grant No. 202103021223072), and the Tencent Foundation or Xplorer Prize. Special thanks should be extended to the Shilawusu Coal Mine and Yankuang Energy Group Company Limited for the provided raw data. The authors thank the anonymous reviewers for constructive comments that helped to improve the quality of the paper.

Conflicts of Interest: The authors declare no conflict of interest.

References

- Xie, H.P.; Ju, Y.; Ren, S.H.; Gao, F.; Liu, J.Z.; Zhu, Y. Theoretical and technological exploration of deep in situ fluidized coal mining. *Front. Energy* **2019**, *13*, 603–611. [\[CrossRef\]](#)
- Dai, L.P.; Pan, Y.S.; Li, Z.H.; Wang, A.W.; Xiao, Y.H.; Liu, F.Y.; Shi, T.W.; Zheng, W.H. Quantitative mechanism of roadway rockbursts in deep extra-thick coal seams: Theory and case histories. *Tunn. Undergr. Sp. Tech.* **2021**, *111*, 103861. [\[CrossRef\]](#)
- Levin, L.A.; Amon, D.J.; Lily, H. Challenges to the sustainability of deep-seabed mining. *Nat. Sustain.* **2020**, *3*, 784–794. [\[CrossRef\]](#)
- Szurgacz, D.; Brodny, J. Analysis of the influence of dynamic load on the work parameters of a powered roof support’s hydraulic leg. *Sustainability* **2019**, *11*, 2570. [\[CrossRef\]](#)
- Fan, D.Y.; Liu, X.S.; Tan, Y.L.; Li, X.B.; Lkhamsuren, P. Instability energy mechanism of super-large section crossing chambers in deep coal mines. *Int. J. Rock Mech. Min. Sci.* **2022**, *32*, 1075–1086. [\[CrossRef\]](#)
- Liu, X.S.; Fan, D.Y.; Tan, Y.L.; Ning, J.G.; Song, S.L.; Wang, H.L.; Li, X.B. New detecting method on the connecting fractured zone above the coal face and a case study. *Rock Mech. Rock Eng.* **2021**, *54*, 4379–4391. [\[CrossRef\]](#)
- Liu, X.S.; Fan, D.Y.; Tan, Y.L.; Song, S.L.; Li, X.F.; Ning, J.G.; Gu, Q.H.; Ma, Q. Failure evolution and instability mechanism of surrounding rock for close-distance parallel chambers with super-large section in deep coal mines. *Int. J. Geomech.* **2021**, *21*, 04021049. [\[CrossRef\]](#)
- Pan, Y.S. Disturbance response instability theory of rockburst in coal mine. *J. China Coal Soc.* **2018**, *43*, 2091–2098.
- He, H.; Dou, L.M.; Gong, S.Y.; He, J.; Zheng, Y.L.; Zhang, X. Microseismic and electromagnetic coupling method for coal bump risk assessment based on dynamic static energy principles. *Safety Sci.* **2019**, *114*, 30–39. [\[CrossRef\]](#)
- Kang, J.Q.; Zhu, J.B.; Zhao, J. A review of mechanisms of induced earthquakes: From a view of rock mechanics. *Geomech. Geophys. Geo-energ. Geo-resour.* **2019**, *5*, 171–196. [\[CrossRef\]](#)
- Bräuner, G. *Rockbursts in Coal Mines and their Prevention*; Routledge: London, UK, 2017.

12. Kuzniar, K.; Tatara, T. The ratio of response spectra from seismic-type free-field and building foundation vibrations: The influence of rockburst parameters and simple models of kinematic soil-structure interaction. *Bull. Earthq. Eng.* **2020**, *18*, 907–924. [[CrossRef](#)]
13. Guo, W.H.; Cao, A.Y.; Wen, Y.Y.; Xue, C.C.; Lv, G.W.; Zhao, Q. Mechanism of rockburst in stopes with typical thick roof and wide coal pillars in Ordos mining area. *J. Min. Saf. Eng.* **2021**, *38*, 720–729.
14. Cao, A.Y.; Chen, F.; Liu, Y.Q.; Dou, L.M.; Wang, C.B.; Yang, X.; Bai, X.X.; Song, S.K. Response characteristics of rupture mechanism and source parameters of mining tremors in frequent coal burst area. *J. China Coal Soc.* **2022**, *47*, 722–733.
15. Pan, J.F.; Qi, Q.X.; Liu, S.H.; Wang, S.W.; Ma, W.T.; Kang, X.C. Characteristics, types and prevention and control technology of rock burst in deep coal mining in China. *J. China Coal Soc.* **2020**, *45*, 111–121.
16. Wang, B.; Jiang, F.X.; Zhu, S.T.; Qu, X.C.; Zhang, X.F.; Wei, Q.D.; Wu, Z.; Xie, H.D. Mechanism and prevention of rock burst induced by segment pillars in the deep mining areas of Shaanxi-Inner Mongolia adjacent regions. *J. Min. Saf. Eng.* **2020**, *37*, 505–513.
17. Wang, B.; Feng, G.R.; Jiang, F.X.; Ma, J.P.; Wang, C.; Li, Z.; Wu, W.W. Investigation into occurrence mechanism of rock burst induced by water drainage in deep mines. *Sustainability* **2023**, *15*, 8891. [[CrossRef](#)]
18. Dou, L.M.; Cai, W.; Cao, A.Y.; Guo, W.H. Comprehensive early warning of rock burst utilizing microseismic multi-parameter indices. *Int. J. Rock Mech. Min. Sci.* **2018**, *28*, 767–774. [[CrossRef](#)]
19. Dou, L.M.; Cao, J.R.; Cao, A.Y.; Chai, Y.J.; Bai, J.Z.; Kan, J.L. Research on types of coal mine tremor and propagation law of shock waves. *Coal Sci. Technol.* **2021**, *49*, 23–31.
20. Cao, A.Y.; Liu, Y.Q.; Chen, F.; Hao, Q.; Yang, X.; Wang, C.B.; Bai, X.X. Focal Mechanism and Source Parameters Analysis of mining-induced earthquakes based on relative moment tensor inversion. *Int. J. Environ. Res. Public Health* **2022**, *19*, 7352. [[CrossRef](#)]
21. Cao, A.Y.; Dou, L.M.; Wang, C.B.; Yao, X.X.; Dong, J.Y.; Gu, Y. Microseismic precursory characteristics of rock burst hazard in mining areas near a large residual coal pillar: A case study from Xuzhuang coal mine, Xuzhou, China. *Rock Mech. Rock Eng.* **2016**, *49*, 4407–4422. [[CrossRef](#)]
22. Orlecka-sikora, B.; Lasocki, S.; Lizurek, G.; Lukasz, R. Response of seismic activity in mines to the stress changes due to mining induced strong seismic events. *Int. J. Rock Mech. Min. Sci.* **2012**, *53*, 151–158. [[CrossRef](#)]
23. Rudzinski, L.; Mirek, K.; Mirek, J. Rapid ground deformation corresponding to a mining-induced seismic event followed by a massive collapse. *Nat. Hazards* **2019**, *96*, 461–471. [[CrossRef](#)]
24. Wu, K.B.; Zou, J.P.; Jiao, Y.Y.; Zhang, X.F.; Wang, C. Focal mechanism of strong ground seismicity induced by deep coal mining. *Rock Mech. Rock Eng.* **2023**, *56*, 779795. [[CrossRef](#)]
25. Mendecki, M.J.; Wojtecki, L.; Zuberek, W.M. Case studies of seismic energy release ahead of underground coal mining before strong tremors. *Pure Appl. Geophys.* **2019**, *176*, 3487–3508. [[CrossRef](#)]
26. He, Z.L.; Lu, C.P.; Zhang, X.F.; Guo, Y.; Meng, Z.H.; Lei, X. Numerical and field investigations of rockburst mechanisms triggered by thick-hard roof fracturing. *Rock Mech. Rock Eng.* **2022**, *55*, 6863–6886. [[CrossRef](#)]
27. Stec, K. Geomechanical conditions of causes of high-energy rock mass tremors determined based on the analysis of parameters of focal mechanisms. *J. Sustain. Min.* **2015**, *14*, 55–65. [[CrossRef](#)]
28. Xue, R.X.; Liang, Z.Z.; Xu, N.W.; Dong, L.L. Rockburst prediction and stability analysis of the access tunnel in the main powerhouse of a hydropower station based on microseismic monitoring. *Int. J. Rock Mech. Min. Sci.* **2020**, *126*, 104174. [[CrossRef](#)]
29. Xu, C.; Fu, Q.; Cui, X.Y.; Zhao, Y.X.; Cai, Y.B. Apparent-depth effects of the dynamic failure of thick hard rock strata on the underlying coal mass during underground mining. *Rock Mech. Rock Eng.* **2019**, *52*, 1565–1576. [[CrossRef](#)]
30. Wu, S.G.; Zhao, Q.; Liu, T. Study on microseismic activity law during change of anti-rockburst coal pillar width. *Coal Sci Technol.* **2020**, *48*, 88–94.
31. Zhu, S.T.; Liu, J.H.; Jiang, F.X.; Shang, X.G.; Sun, X.K.; Zhang, X.F.; Song, D.Z.; Zhang, M.; Wang, A.W.; Xie, H.D.; et al. Classification, prediction, prevention and control of roof movement-type mine earthquakes and induced disasters in China's coal mines. *J. China Coal Soc.* **2022**, *47*, 807–816.
32. Shan, X.G.; Zhu, S.T.; Jiang, F.X.; Liu, J.H.; Zhang, X.F.; Sun, X.; Wang, C.; Chen, Y.; Xu, B.; Li, J.J.; et al. Study on mine earthquakes mechanism and ground vertical well hydraulic fracturing shock absorption in thick hard rock mine. *Sustainability* **2023**, *15*, 5122.
33. Shan, X.G.; Zhu, S.T.; Jiang, F.X.; Liu, J.H.; Li, J.J.; Hitch, M.; Liu, H.L.; Tang, S.B.; Zhu, C. Study on dynamic disaster mechanisms of thick hard roof induced by hydraulic fracturing in surface vertical well. *Minerals* **2022**, *12*, 1537.
34. Cui, F.; Yang, Y.B.; Lai, X.P.; Cao, J.T. Similar material simulation experimental study on rockbursts induced by key stratum breaking based on microseismic monitoring. *Chin. J. Rock Mech. Eng.* **2019**, *38*, 803–814.
35. Lai, X.P.; Jia, C.; Cui, F.; Zhang, N.; Chen, J.Q.; Sun, J.X.; Zhang, S.L.; Feng, G.G. Study on the evolution law of overburden energy of steeply inclined extra-thick coal seam influenced by mining depth. *Chin. J. Rock Mech. Eng.* **2023**, *42*, 261–274.
36. Gao, M.S.; Xu, D.; He, Y.L.; Zhang, Z.G.; Yu, X. Investigation on the near-far field effect of rock burst subject to the breakage of thick and hard overburden. *J. Min. Saf. Eng.* **2022**, *39*, 215–226.
37. Yu, B.; Gao, R.; Meng, X.B.; Kuang, T.J. Near-far strata structure instability and associate strata behaviors in large space and corresponding control technology. *Chin. J. Rock Mech. Eng.* **2018**, *37*, 1134–1145.
38. Gao, R.; Kuang, T.J.; Zhang, Y.Q.; Zhang, W.Y.; Quan, C.Y. Controlling mine pressure by subjecting high-level hard rock strata to ground fracturing. *Int. J. Coal Sci. Technol.* **2021**, *8*, 1336–1350. [[CrossRef](#)]

39. Qin, Z.H.; Chen, C.Q.; Li, F.H.; Zhang, Y.; Du, T.T. Seismic mechanism and prevention technology of solid coal roadway in deep buried structural area. *Coal Sci. Tech.* **2021**, *49*, 87–92.
40. Wen, Y.Y.; Guo, Z.G.; Cao, A.Y.; Wang, S.W.; Bai, X.X.; Jiang, S.Q. Analysis of pressure relief effect of roof deep hole blasting parameters based on micro-seismic data evaluation. *Coal Sci. Tech.* **2020**, *48*, 57–63.
41. Pan, J.F.; Kang, H.P.; Yan, Y.D.; Ma, X.H.; Ma, W.T.; Lu, C.; Lv, D.Z.; Xu, G.; Feng, M.H.; Xia, Y.X.; et al. The method, mechanism and application of preventing rockburst by artificial liberation layer of roof. *J. China Coal Soc.* **2023**, *48*, 636–648.
42. Cao, A.Y.; Dou, L.M.; Cai, W.; Gong, S.Y.; Liu, S.; Jing, G.C. Case study of seismic hazard assessment in underground coal mining using passive tomography. *Int. J. Rock Mech. Min. Sci.* **2015**, *78*, 1–9. [[CrossRef](#)]
43. Qian, M.G.; Miao, X.X.; Xu, J.L. Theoretical study of key stratum in ground control. *J. China Coal Soc.* **1996**, *24*, 225–230.
44. Qian, M.G.; Shi, P.W.; Xu, J.L. *Mine Pressure and Ground Control*; China University of Mining and Technology Press: Xuzhou, China, 2010; pp. 176–230.
45. Niu, Y.; Li, Z.H.; Wang, E.Y.; Shan, T.C.; Wang, H.; Xu, S.L.; Sun, W.Y.; Wang, G.T.; Xue, X.Z.; Liu, J.Q. Response characteristics of electric potential and its relationship with dynamic disaster during mining activities: A case study in Xuehu Coal Mine, China. *Int. J. Environ. Res. Public Health* **2022**, *19*, 8949. [[CrossRef](#)] [[PubMed](#)]
46. Jiang, F.X.; Liu, Y.; Zhang, Y.C.; Wen, J.L.; Yang, W.L.; An, J. A three-zone structure loading model of overlying strata and its application on rockburst prevention. *Chin. J. Rock Mech. Eng.* **2016**, *35*, 2398–2408.
47. Holla, L. Ground movement due to longwall mining in high relief areas in New South Wales, Australia. *Int. J. Rock Mech. Min. Sci.* **1997**, *34*, 775–787. [[CrossRef](#)]
48. Li, Z.; Yu, S.C.; Zhu, W.B.; Feng, G.R.; Xu, J.M.; Guo, Y.X.; Qi, T.Y. Dynamic loading induced by the instability of voussoir beam structure during mining below the slope. *Int. J. Rock Mech. Min. Sci.* **2020**, *132*, 104343. [[CrossRef](#)]
49. Hudyma, M.; Potvin, Y. An engineering approach to seismic risk management in hard rock mines. *Rock Mech. Rock Eng.* **2010**, *43*, 891–906. [[CrossRef](#)]
50. Cui, F.; Zhang, T.H.; Lai, X.P.; Wang, S.J.; Chen, J.Q.; Qian, D.Y. Mining disturbance characteristics and productivity of rock burst mines under different mining intensities. *J. China Coal Soc.* **2021**, *46*, 3781–3793.
51. Feng, L.F.; Dou, L.M.; Wang, X.D.; Jin, D.W.; Cai, W.; Xu, G.G.; Jiao, B. Mechanism of mining advance speed on energy release from hard roof movement. *J. China Coal Soc.* **2019**, *44*, 3329–3339.
52. Gong, F.Q.; Zhang, P.L.; Luo, S.; Li, J.C.; Huang, D. Theoretical damage characterisation and damage evolution process of intact rocks based on linear energy dissipation law under uniaxial compression. *Int. J. Rock Mech. Min. Sci.* **2021**, *146*, 104858. [[CrossRef](#)]
53. Hosseini, N. Evaluation of the rock burst potential in longwall coal mining using passive seismic velocity tomography and image subtraction technique. *J. Seismol.* **2017**, *21*, 1101–1110. [[CrossRef](#)]
54. Li, F.; Wang, C.C.; Sun, R.C.; Xiang, G.Y.; Ren, B.R.; Zhang, Z. Frequency response characteristics and failure model of single-layered thin plate rock mass under dynamic loading. *Sci. Rep.* **2022**, *12*, 19047. [[CrossRef](#)]
55. Jiang, F.X.; Zhang, X.; Zhu, S.T. Discussion on key problems in prevention and control system of coal mine rock burst. *Coal Sci. Tech.* **2023**, *51*, 203–213.
56. Xuan, D.Y.; Xu, J.L.; Wang, B.L. Green mining technology of overburden isolated grout injection. *J. China Coal Soc.* **2022**, *47*, 4265–4277.
57. Xuan, D.Y.; Wang, B.L.; Xu, J.L. A shared borehole approach for coal-bed methane drainage and ground stabilization with grouting. *Int. J. Rock Mech. Min. Sci.* **2016**, *86*, 235–244. [[CrossRef](#)]

Disclaimer/Publisher’s Note: The statements, opinions and data contained in all publications are solely those of the individual author(s) and contributor(s) and not of MDPI and/or the editor(s). MDPI and/or the editor(s) disclaim responsibility for any injury to people or property resulting from any ideas, methods, instructions or products referred to in the content.